TECHNISCHE MECHANIK
an open access journal

journal homepage: www.ovgu.de/techmech

Tech. Mech., Vol. 42, Is. 1, (2022), 66–74

Received: 07.06.2022
Accepted: 02.12.20222
Available online: 13.12.2022

Analytical model of wave propagation in piezo thermo elastic multilayered PZT5A/LEMV/SWCNT/LEMV/PZT5A circular cylinder

S. Mahesh[1] R. Selvamani[2]*

[1] V.S.B.Engineering College,Department of Mathematics,Karur,TamilNadu, India.
[2] Karunya University,Department of Mathematics,Coimbatore ,TamilNadu, India.

Abstract: In this study we revised the axisymmetric vibration of an infinite thermo piezoelectric composite circular hollow cylinder made of inner and outer thermo piezoelectric layer bonded together by a Linear Elastic Material with Voids (LEMV) and Single Walled carbon Nano Tube (SWCNT) is studied. The frequency equations are obtained for the traction free outer surface with continuity conditions at the interfaces. The equations of motion, heat and electric conduction also exactly solved. Numerical results are carried out for the inner and outer hollow piezoelectric layers bonded by LEMV and SWCNT layers. The dispersion curves are compared with core/LEMV/core, core cylinders.

Keywords: Composite hollow cylinder, LEMV, SWCNT, Dispersion relation, Bessels function.

1 Introduction

An enormous number of lively vibration mechanism perceptions have grown over the past few decades to achieve enhanced vibration suppression of structures and adapt to changes in the excitation and structural properties. Instead, a range of semi-active damping control conceptions have evolved for numerous structural vibration control applications, which could offer performance gains comparable to those of the active control devices with only minimal power requirement. In ongoing decades, the utilization of Nano composite structures has been developing quickly and has pulled in much consideration from logical examination networks. Among the used nanofillers, CNT and graphene have gotten well known because of their extraordinary thermo-mechanical properties. Vibration and wave engendering of carbon nanotubes (CNTs) are as of late pulling in a developing enthusiasm because of their different applications in nanoscale gadgets, superconductivity, transport and optical wonders. In spite of the fact that few atomistic models have been effectively used to get the vibrational qualities of CNTs, the related computational expense supports continuum displaying which is likewise discovered to be calculable.
Upadhya et al. (2018) exposed the modified fourier heat flux on MHD flow over stretched cylinder filled with dust, graphene and silver nanoparticles. Moradi-Dastjerdi and Behdinan (2019) scrutinized thermoelastic static and vibrational behaviors of nanocomposite thick cylinders reinforced with graphene. Wang et al. (2014a) deliberate Multifunctional graphene sheet–nanoribbon hybrid aerogels.Sobhy (2016) revealed hygrothermal vibration of orthotropic double-layered graphene sheets embedded in an elastic medium using the two-variable plate theory.Garg et al. (2014) explored an embedded simulation approach for modeling the thermal conductivity of 2D nanoscale material.Liew et al. (2006) scrutinized Predicting nanovibration of multi-layered graphene sheets embedded in an elastic matrix.Ansari et al. (2011) revealed Vibration characteristics of embedded multi-layered graphene sheets with different boundary conditions via nonlocal elasticity.Wang et al. (2011) studied Geometrical nonlinear free vibration of multi-layered graphene sheets.Sakhaee-Pour et al. (2008) exposed Vibrational analysis of single-layered graphene sheets.Wang et al. (2014b) conversed free vibration analysis of single-layered graphene sheets based on a continuum model. Generalized two-variable plate theory for multi-layered graphene sheets with arbitrary boundary conditions deliberate by Sobhy (2014). Influence of initial shear stress on the vibration behavior of single-layered graphene sheets embedded in an elastic medium based on Reddy's higher-order shear deformation plate theory debated by Ebrahimi and Shafiei (2017).Bakhshalizadeh and Ghadiri (2020) evaluated Size-dependent vibration behavior of graphene sheet with attached spring-mass and damper system based on the nonlocal Eringen theory.Mazur and Awrejcewicz (2020) expressed Ritz Method in Vibration Analysis for Embedded Single-Layered Graphene Sheets Subjected to In-Plane Magnetic Field. A Novel Method for Considering Interlayer Effects between Graphene Nanoribbons and Elastic Medium in Free Vibration Analysis studied by Kamali and Nazemnezhad (2020).Analooei et al. (2020) discussed on the vibration and buckling analysis of quadrilateral and triangular nanoplates using nonlocal spline finite strip method.Behdinan et al. (2020) [17] discussed Graphene and CNT impact on heat transfer response of nanocomposite cylinders.Ebrahimi et al. (2021) studied buckling analysis of embedded graphene oxide powder-reinforced nanocomposite shells.Moradi-Dastjerdi and Behdinan (2020) discussed Stability analysis of multifunctional smart sandwich plates with graphene nanocomposite and porous layers.Ebrahimi and Dabbagh (2020) discussed Viscoelastic wave propagation analysis of axially motivated double-layered graphene sheets via nonlocal strain gradient theory.Fouaidi et al. (2021) discussed Numerical analysis of single-layered graphene sheets by a mesh-free approach. Bellal et al. (2020) analyses Buckling behavior of a single-layered graphene sheet resting on

* E-mail address: selvam1729@gmail.com
doi: 10.24352/UB.OVGU-2022-061

viscoelastic medium via nonlocal four-unknown integral model.Shafiei et al. (2020) discovery application of modified couple-stress theory to stability and free vibration analysis of single and multi-layered graphene sheets. Xu et al. (2020) discussed flexural Wave Propagation of Double-Layered Graphene Sheets Based on the Hamiltonian System.
In this examination we restructured the axisymmetric vibration of an infinite thermo piezoelectric composite circular hollow cylinder made of inward and external thermo piezoelectric layer fortified together by a LEMV and SWCNT is considered. The frequency equations are acquired for the traction free external surface with continuity conditions at the interfaces. A Bessel function solution with complex argument is directly used to analyze the frequency equations. The computed non-dimensional frequencies are plotted in the form of dispersion curves against the wave number, voltage difference and linear temperature change. The numerical results are compared with different combinations of hollow cylinders.

2 PROBLEM FORMULATION

In this section we consider an infinite thermo piezoelectric composite circular hollow cylinder made of inner and outer thermo piezoelectric layer bonded together by a LEMV and SWCNT.In cylindrical coordinates (r, z), the equations of motion in axisymmetric direction and absence of body force

$$\sigma^l_{rr,r} + \sigma^l_{rz,z} + r^{-1}\sigma^l_{,rr} = \rho u_{,tt} \tag{1a}$$
$$\sigma^l_{rz,r} + \sigma^l_{zz,z} + r^{-1}\sigma^l_{,rz} = \rho w_{,tt} \tag{1b}$$

The electric displacement equation is given as

$$\frac{1}{r}\frac{\partial}{\partial r}(rD^l_r) + \frac{\partial}{\partial z}(D^l_z) = 0 \tag{2}$$

The heat conduction equation is defined as

$$K_{11}(T^l_{,rr} + r^{-1}T^l_{,r} + r^{-2}T^l_{,\theta\theta}) + K_{33}T^l_{,zz} - \rho^l c_v T_{,t} = T_0\frac{\partial}{\partial t}[\beta_1(e^l_{,rr} + e^l_{,\theta\theta}) + \beta_3 e^1_{,zz} - p_3\phi_{,z}] \tag{3}$$

Relation between the stress and strain of mechanical and electrical field is

$$\sigma^l_{rr} = c_{11}e^l_{rr} + c_{12}e^l_{\theta\theta} + c_{13}e^l_{zz} - \beta_1 T^l - e_{31}E^l_z \tag{4a}$$
$$\sigma^l_{zz} = c_{13}e^l_{rr} + c_{13}e^l_{\theta\theta} + c_{33}e^l_{zz} - \beta_3 T^l - e_{33}E^l_z \tag{4b}$$
$$\sigma^l_{rz} = c_{44}e^l rz \tag{4c}$$
$$D_r = e_{15}e^l_{rz} + \varepsilon_{11}E^l_r \tag{4d}$$
$$D_z = e_{31}(e^l_{rr} + e^l_{\theta\theta}) + e_{33}e^l_{zz} + \varepsilon_{33}E^l_z + p_3 T \tag{4e}$$

where $\sigma^l_{rr}, \sigma^l_{r\theta}, \sigma^l_{rz}, \sigma^l_{\theta\theta}, \sigma^l_{zz}, \sigma^l_{z\theta}$ denotes mechanical stress component, $e^l_{\theta\theta}, e^l_{r\theta}, e^l_{z\theta}, e^l_{rz}$ are the strain components, T^l is the temperature change about the equilibrium temperature,$c_{11}, c_{12}, c_{13}, c_{33}, c_{44}, c_{66}$ are the five elastic constants,β_1, β_3 and K_1, K_3 respectively thermal expansion coefficients and thermal conductivities along and perpendicular to the symmetry, ρ is the mass density, c_v is the specific heat capacity,p_3 is the pyroelectric effect.
The strains e_{ij} are related to the displacements given by

$$e^l_{rr} = u^l_{,r} e^l_{\theta\theta} = r^{-1}(u^l + v^l_{,\theta}), e^l_{zz} = w^l_{,rz} \tag{5a}$$
$$e^l_{r\theta} = v^l_r - r^{-1}(v^l - u^l_{,\theta}), \tag{5b}$$
$$e^l_{z\theta} = v^l_{,z} + r^{-1}w^l_{,r\theta} e^l_{rz} = w^l_{,r} + u^l_{,z} \tag{5c}$$

Substitution of the (4) and (5) into (1) to (3) results in the following three dimensional equation of motion,electric and heat conduction:

$$c_{11}(u^l_{,rr} + r^{-1}u^l_{,r} + r^{-2}u^l) + c_{44}u^l_{,zz} + (c_{44} + c_{13})w^l_{rz} + (e_{31} + e_{15})E^l_{rz} - \beta_1 T^l_{,r} + = \rho u^l_{,tt} \tag{6a}$$

$$c_{44}(w^l_{rr} + r^{-1}w^l_{,r}) + r^{-1}(c_{44} + c_{13})u^l_{,z} + (c_{44} + c_{13})u^l_{,rz} + c_{33}w^l_{,zz} + e_{33}E_{,zz}(E_{,rr} + r^{-1}E_{,r}) - \beta_3 T_{,z} = \rho w^l_{,tt} \tag{6b}$$

$$e_{15}(w^l_{rr} + r^{-1}w^l_{,r}) + e_{31} + e_{15}(u^l_{,rz} + r^{-1}u^l_{,z}) + e_{33}w^l_{,zz} - \eta_{33}E^l_{,zz} - \eta_{11}(E^l_{,rr} + r^{-1}E^l_{,r}) + p_3 T^l_{,z} = 0 \tag{6c}$$

$$K_{11}(T^l_{,rr} + r^{-1}T^l_{,r} + r^{-2}T^l_{,\theta\theta}) + K_{33}T^l_{,zz} - \rho^l c_v T_{,t} = T_0\frac{\partial}{\partial t}[\beta_1(u^l_{,r} + r^{-1}v^l_{,\theta} + r^{-1}u^l) + \beta_3 w^l_{,z}] - p_3 E^l_{,z} \tag{6d}$$

Solution of the above field Equation Selvamani and Mahesh (2019)

$$u^l(r,z,t) = (U^l_{,r}) \exp i(kz+\omega t) \tag{7a}$$

$$w^l(r,z,t) = \frac{i}{a} W^l \exp i(kz+\omega t) \tag{7b}$$

$$E^l(r,z,t) = \frac{ic_{44}}{ae_{33}} E^l \exp i(kz+\omega t) \tag{7c}$$

$$T^l(r,z,t) = \frac{c_{44}}{\beta_3 a^2} T^l \exp i(kz+\omega t) \tag{7d}$$

Here $i = \sqrt{-1}$, k is the wave number,ω is the frequency U^l, W^l, E^l, T^l are all displacement potentials, electric conduction and thermal change. By introducing the dimensionless quantities such as $x = \frac{r}{a}$,$\eta = ka$, $\Omega^2 = \frac{\rho\omega^2 a^2}{c_{44}}$,$\bar{c}_{11} = \frac{c_{11}}{c_{44}}$,
$\bar{c}_{13} = \frac{c_{13}}{c_{44}}$,$\bar{c}_{33} = \frac{c_{33}}{c_{44}}$,$\bar{c}_{66} = \frac{c_{66}}{c_{44}}$,$\bar{\beta} = \frac{\beta_1}{\beta_3}$,$\bar{k}_i = \frac{(\rho c_{44})^{\frac{1}{2}}}{\beta_3^2 T_0 a\Omega}$,$\bar{d} = \frac{\rho c_v c_{44}}{\beta_3^2 T_0}$,$\bar{p}_3 = \frac{p_3 c_{44}}{\beta_3 e_{33}}$
Substituting (7) in (6) we obtain

$$(\bar{c}_{11}\nabla^2 + (\Omega^2 - \zeta^2))U^l - \zeta(1+\bar{c}_{13})W^l - \zeta(\bar{e}_{31}+\bar{e}_{15})E^l - \bar{\beta}T^l = 0 \tag{8a}$$

$$\zeta(1+\bar{c}_{13})\nabla^2 U^l + (\nabla^2 + (\Omega^2 - \zeta^2\bar{c}_{33}))W^l + (\bar{e}_{33}\nabla^2 - \zeta^2)E^l - \zeta T^l = 0 \tag{8b}$$

$$\zeta(\bar{e}_{31}+\bar{e}_{15})\nabla^2 U^l + (\bar{e}_{15}\nabla^2 - \zeta^2)W^l + (\zeta^2\bar{\epsilon}_{33} - \bar{\epsilon}\nabla^2)E^l + \zeta\bar{p}_3 T^l = 0 \tag{8c}$$

$$\bar{\beta}\nabla^2 U^l - \zeta W^l + \zeta\bar{p}_3 E^l + (\bar{d} + i\bar{k}_1\nabla^2 + i\bar{k}_3\zeta^2)T^l = 0 \tag{8d}$$

where $\nabla^2 = \frac{\partial^2}{\partial x^2} + x^{-1}\frac{\partial}{\partial x}$

$$\begin{vmatrix} [\bar{c}_{11}\nabla^2 + (\Omega^2 - \zeta^2)] & -\zeta(1+\bar{c}_{13}) & \zeta(\bar{e}_{31}+\bar{e}_{15}) & -\bar{\beta} \\ \zeta(1+\bar{c}_{13})\nabla^2 & [\nabla^2 + (\Omega^2 - \bar{c}_{33}\zeta^2)] & (\bar{e}_{33}\nabla^2 - \zeta^2) & -\zeta \\ \zeta(\bar{e}_{31}+\bar{e}_{15})\nabla^2 & \bar{e}_{15}\nabla^2 - \zeta^2 & (\zeta^2\bar{\epsilon}_{33} - \bar{\epsilon}\nabla^2) & \zeta\bar{p}_3 \\ \bar{\beta}\nabla^2 & -\zeta & \zeta\bar{p}_3 & (\bar{d} + i\bar{k}_1\nabla^2 - i\bar{k}_3\zeta^2) \end{vmatrix} (U^l, W^l, E^l, T^l)^T = 0 \tag{9}$$

Evaluating the given in (9), we obtain a partial differential equation of the form

$$(A^l\nabla^8 + B^l\nabla^6 + C^l\nabla^4 + D^l\nabla^2 + E^l)(U^l, W^l, E^l, T^l)^T = 0 \tag{10}$$

Factorizing the relation given in (10) into biquadrate equation for $(\alpha_j^2 a)^2, j = 1,2,3,4$ the solutions for the symmetric modes are obtained as

$$U^l = \sum_{j=1}^{4} [A_j J_n(\alpha_j x) + B_j y_n(\alpha_j x)], \tag{11a}$$

$$W^l = \sum_{j=1}^{4} a_j^l [A_j J_n(\alpha_j x) + B_j y_n(\alpha_j x), \tag{11b}$$

$$E^l = \sum_{j=1}^{4} b_j^l [A_j J_n(\alpha_j x) + B_j y_n(\alpha_j x)], \tag{11c}$$

$$T^l = \sum_{j=1}^{4} c_j^l [A_j J_n(\alpha_j x) + B_j y_n(\alpha_j x)], \tag{11d}$$

Here $(\alpha_j^l ax) > 0, for (j = 1,2,3,4)$ are the roots of algebraic equation

$$(A^l(\alpha_j^l ax)^8 + B^l(\alpha_j^l ax)^6 + C^l(\alpha_j^l ax)^4 + D^l(\alpha_j^l ax)^2 + E^l)(\phi^l, W^l, E^l, T^l)^T = 0$$

Here a_j^l, b_j^l, c_j^l are the arbitrary constants and $J_n(\alpha_l^j ax)$ denotes the Bessel functions first kind of order n. The constants a_j^l, b_j^l, c_j^l are calculated using the following relations with $\nabla^2 = \alpha_j^l ax$

$$(\bar{c}_{11}\nabla^2 + (\Omega^2 - \zeta^2)) - \zeta(1+\bar{c}_{13})a_j^l - \zeta(\bar{e}_{31}+\bar{e}_{15})b_j^l - \bar{\beta}c_j^l = 0$$

$$\zeta(1+\bar{c}_{13})\nabla^2 + (\nabla^2 + (\Omega^2 - \zeta^2\bar{c}_{33}))a_j^l + (\bar{e}_{33}\nabla^2 - \zeta^2)b_j^l - \zeta c_j^l = 0$$

$$\zeta(\bar{e}_{31}+\bar{e}_{15})\nabla^2 + \bar{e}_{15}\nabla^2 - \zeta^2)a_j^l + \zeta\bar{p}_3 b_j^l + (\zeta^2\bar{\epsilon}_{33} - \bar{\epsilon}\nabla^2)c_j^l = 0$$

$$\bar{\beta}\nabla^2 - \zeta a_j^l + (\bar{d} + i\bar{k}_3\zeta^2)b_j^l + \zeta\bar{p}_3 c_j^l = 0$$

3 EQUATION OF MOTION FOR LINEAR ELASTIC MATERIALS WITH VOIDS

The equations of motion for isotropic LEMV materials are given as Cowin and Nunziato (1983)

$$(\lambda+2\mu)(u_{,rr}+r^{-1}u_{,r}-r^{-2}u)+\mu u_{,zz}+(\lambda+\mu)w_{,zz}+\beta\chi_{,r}=\rho u_{,tt} \tag{12a}$$

$$(\lambda+\mu)(u_{,rz}+r^{-1}u_{,z})+\mu(w_{,rr}+r^{-1}w_{,r})+(\lambda+2\mu)w_{,zz}+\beta\chi_{,z}=\rho w_{,tt} \tag{12b}$$

$$-\beta(u_{,r}+r^{-1}u)-\beta w_{,z}+\alpha(\chi_{,rr}+r^{-1}\chi_{,r}+\chi_{,zz})-\delta k\chi_{,tt}-\omega\chi_{,t}-\xi\chi=0 \tag{12c}$$

u,w represents displacements components along $randz$ directions α,β,ξ,ω and k are LEMV material constants characterizing the core in the equilibrated inertial state,ρ is the density and λ,μ are the lame constants and χ is the new kinematical variable associated with another material without voids. The stress in the LEMV core materials are

$$\sigma_{,rr}=(\lambda+2\mu)u_{,r}+\lambda r^{-1}u+\lambda w_{,z}+\beta\chi$$
$$\sigma_{,rz}=\mu(u_{,t}+w_{,r})$$

The solution of for (12) is taken as

$$u=\quad \mathcal{U}_{,r}\exp i(kz+pt) \tag{13a}$$

$$w=(\frac{i}{h})\mathcal{W}\exp i(kz+pt) \tag{13b}$$

$$\chi=(\frac{1}{h^2})\boldsymbol{\chi}\exp i(kz+pt) \tag{13c}$$

The above solution in (13) and dimensionless variables x and ε, equation(12) can be reduced as

$$\begin{vmatrix}(\lambda+2\mu)\nabla^2+M_1 & -M_2 & M_3\\ M_2\nabla^2 & \bar{\mu}\nabla^2+M_4 & M_5\\ -M_3\nabla^2 & M_5 & \alpha\nabla^2+M_6\end{vmatrix}(\mathcal{U},\mathcal{W},\boldsymbol{\chi})^T=0 \tag{14}$$

where $\nabla^2=\frac{\partial^2}{\partial x^2}+\frac{1}{x}\frac{\partial}{\partial x}$, $M_1=\frac{\rho}{\rho^1}(ch)^2-\bar{\mu}\varepsilon^2$,$M_2=(\bar{\lambda}+\bar{\mu})\varepsilon$,$M_3=\bar{\beta}$, $M_4=\frac{\rho}{\rho^1}(ch)^2-(\bar{\lambda}+\bar{\mu})\varepsilon^2$,
$M_5=\bar{\beta}\varepsilon$, $M_6=\frac{\rho}{\rho^1}(ch)^2\bar{k}-\bar{\alpha}\varepsilon^2-i\bar{\omega}(ch)-\bar{\xi}$

The Equation (14) can be specified as,

$$(\nabla^6+P\nabla^4+Q\nabla^2+R)(\mathcal{U},\mathcal{W},\boldsymbol{\chi})=0 \tag{15}$$

Thus the solution of Equation (15) is as follows,

$$\mathcal{U}=\quad\sum_{j=1}^{3}[A_jJ_0(\alpha_jx)+B_jy_0(\alpha_jx)] \tag{16a}$$

$$\mathcal{W}=\sum_{j=1}^{3}d_j[A_jJ_0(\alpha_jx)+B_jy_0(\alpha_jx)], \tag{16b}$$

$$\boldsymbol{\chi}=\sum_{j=1}^{3}e_j[A_jJ_0(\alpha_jx)+B_jy_0(\alpha_jx)] \tag{16c}$$

$(\alpha_jx)^2$ are zeros of the equation when replacing $\nabla^2=-(\alpha_jx)^2$. The arbitrary constant d_j and e_j are obtained from

$$M_2\nabla^2+(\bar{\mu}\nabla^2+M_4)d_j+M_5e_j=0$$
$$-M_3\nabla^2+M_5d_j+(\alpha\nabla^2+M_6)e_j=0$$

For the governing equation of CFRP core material, we assume void volume fraction $\chi=0$, and the lame's constants as $\lambda=c_{12},\mu=\frac{c_{11}-c_{12}}{2}$ in the Equation(12)

4 Mathematical formulations for SWCNT

The governing elasto-dynamic equation for a SWCNT is given as Mitra and Gopalakrishnan (2007)

$$(\Lambda+2M)(\mathfrak{u}^l_{,rr}+r^{-1}\mathfrak{u}^l_{,r}-r^{-2}\mathfrak{u}^l)+M\mathfrak{u}^l_{,zz}+(\Lambda+M)\mathfrak{w}^l_{,zz}=\acute{\rho}\mathfrak{u}^l_{,tt} \tag{17a}$$

$$(\Lambda+M)(\mathfrak{u}^l_{,rz}+r^{-1}\mathfrak{u}^l_{,z})+M(\mathfrak{w}^l_{,rr}+r^{-1}\mathfrak{w}^l_{,r})+(\Lambda+2M)\mathfrak{w}^l_{,zz}+=\acute{\rho}\mathfrak{w}^l_{,tt} \tag{17b}$$

$$\tag{17c}$$

Here $\mathfrak{u}^l$ is the displacement vector, $\Lambda^l = C_{12}, M^l = (C_{11} - C_{12})/2$ are Lames constants
$\acute{\rho^l}$ is the mass density and t is time. The solution of above equation is taken as

$$\mathfrak{u}^l = \quad \mathfrak{U}^l_{,r} \exp i(kz + pt) \tag{18a}$$

$$\mathfrak{w}^l = (\frac{i}{h})\mathfrak{W}^l \exp i(kz + pt) \tag{18b}$$

Using the solution in and dimensionless variables x and ϵ, equation (17) can be simplified as

$$\begin{vmatrix} (\bar{\Lambda} + 2\bar{M})\nabla^2 + H_1^l & -H_2 \\ H_2^l & \bar{M}\nabla^2 + H_3^l \end{vmatrix} (\mathfrak{U}^l, \mathfrak{W})^T = 0 \tag{19}$$

where $\bar{\Lambda} = \frac{\Lambda^l}{C_{44}^1}$, $\bar{M}^l = \frac{M^l}{C_{44}^1}$, $H_1^l = \frac{\rho^l}{\rho^1}(ch)^2 - \bar{M}^l\epsilon^2$, $H_2^l = (\bar{\Lambda}^l + \bar{M}^l)\epsilon^2$, $H_3^l = \frac{\rho^l}{\rho^1}(ch)^2 - (\bar{\Lambda}^l + 2\bar{M}^l)\epsilon^2$

The equation (19) can be written as

$$(\nabla^4 + P^l\nabla^2 + Q^l)(\mathfrak{U}^l, \mathfrak{W}^l) = 0 \tag{20}$$

The solution of (20) is

$$\mathfrak{U}^l = \sum_{j=1}^{3}[A_j J_0(\alpha_j x) + B_j y_0(\alpha_j x)] \tag{21a}$$

$$\mathfrak{W}^l = \sum_{j=1}^{3} f_j^l [A_j J_0(\alpha_j x) + B_j y_0(\alpha_j x)] \tag{21b}$$

Where $(\alpha_j^l)^2$ is nonzero roots of

$$((\alpha_j^l)^4 + P^l(\alpha_j^l)^2 + Q^l)(\mathfrak{U}^l, \mathfrak{W}^l) = 0 \tag{22}$$

And the arbitrary constants f_j^l are obtained from

$$f_j^l = \frac{[-(\bar{\Lambda}^l + 2\bar{M}^l)(\alpha_j^l)^2]}{H_2^l} \tag{23}$$

5 BOUNDARY CONDITIONS AND FREQUENCY EQUATIONS

The frequency equation can be obtained by using the following boundary and interface conditions
(i) On the traction free inner surface
$\sigma_{rr}^l = \sigma_{rz}^l = E^l = T^l = 0$ With $l = 1$.
(ii) At the interface $\sigma_{rr}^l = \sigma_{rr}; \sigma_{rz}^l = \sigma_{rz}; E^l = T^l = D^l = 0$
Substituting the above boundary condition we obtained as a 32×32 determinant equation

$$|(Y_i j)| = 0, (i, j = 1, 2, 3, ..., 32) \tag{24}$$

At $x = x_0$ *where* $j = 1, 2, 3, 4$

$$\aleph(1, j) = 2\bar{c}_{66}\left(\frac{\alpha_j}{x_0}\right)\mathscr{J}_1(\alpha_j^1 x_0) - [(\bar{c}_{11})(\epsilon_j^1 a)^2 + \bar{c}_{13}\epsilon a_j^1 + \bar{e}_{31}\epsilon b_j^1 + \bar{q}_{31}c_j^1]\mathscr{J}_0(\alpha_j^1 x_0)$$

$$\begin{aligned} \aleph(2, j) &= (\epsilon + a_j^1 + \bar{e}_{15}b_j^1)(\alpha_j^1)\mathscr{J}_1(\alpha_j^1 x_0), \\ \aleph(3, j) &= b_j^1\mathscr{J}_0(\alpha_j^1 x_0) \\ \aleph(4, j) &= \frac{c_j^1}{x_0}\mathscr{J}_0(\alpha_j^1 x_0) - (\alpha_j^1)\mathscr{J}_1(\alpha_j^1 x_0), \end{aligned}$$

In addition, the other nonzero elements $Y_{1,j+4}, Y_{2,j+4}, Y_{3,j+4}$ and $Y_{4,j+4}$ are obtained by replacing J_0 by $J_1$and R_0 by R_1.
At $x_1 = \frac{a_1}{a}$,

$$\aleph(5, j) = \bar{c}_{66}(\frac{\alpha_j}{x_1})\mathscr{J}_1(\alpha_j^1 x_1) - [(\bar{c}_{11})(\epsilon_j^1 a)^2 + \bar{c}_{13}\epsilon a_j^1 + \bar{e}_{31}\epsilon b_j^1 + \bar{q}_{31}c_j^1]\mathscr{J}_0(\alpha_j^1 x_1)$$

$$\aleph(5, j + 8) = 2\mu(\frac{\alpha_j}{x_1})\mathscr{J}_1(\alpha_j x_1) + [-(\bar{\lambda} + 2\bar{\mu})(\alpha_j^2) + \bar{q}_{31}b_j^1 - \bar{\lambda}\epsilon$$

$$
\begin{aligned}
\aleph(6,j) &= (\epsilon + a_j^1 + \bar{e}_{15} b_j^1)(\alpha_j^1)\, \mathscr{J}_1(\alpha_j^1 x_1),\\
\aleph(6,j+8) &= -\mu((\epsilon + a_j^1))(\alpha_j^1)\, \mathscr{J}_1(\alpha_j^1 x_1)\\
\aleph(7,j) &= (\alpha_j^1)\, \mathscr{J}_1(\alpha_j^1 x_1),\\
\aleph(7,j+8) &= -(\alpha_j^1)\, \mathscr{J}_1(\alpha_j^1 x_1),\\
\aleph(8,j) &= a_j^1\, \mathscr{J}_0(\alpha_j^1 x_1),\\
\aleph(8,j+8) &= -a_j^1\, \mathscr{J}_0(\alpha_j^1 x_1),\\
\aleph(9,j) &= b_j^1\, \mathscr{J}_0(\alpha_j^1 x_1)\\
\aleph(10,j) &= b_j^1 \alpha_j\, \mathscr{J}_0(\alpha_j^1 x_1\\
\aleph(11,j) &= \frac{c_j^1}{x_1}\, \mathscr{J}_0(\alpha_j^1 x_1) - (\alpha_j^1)\, \mathscr{J}_1((\alpha_j^1 x_1))
\end{aligned}
$$

and the remaining nonzero element $\aleph(i,j)$ can be obtained on replacing J_0 by J_1 and Y_0 by Y_1 in the above elements.where $i = 5,6,\ldots,11, j = 5,6,7,8$ in the Similar way $\aleph(i,11+k)$ also obtained where $k = 5,6,7,8$.
At the interfaces $x_2 = \frac{a_2}{a}$ non-zero elements along the following are obtained on replacing x_1 by x_2 and super script 1 by 2 in order. Here $j = 7,8$ and $k = 6,7,8$.

$$
\begin{aligned}
\aleph(12,j) &= 2\bar{M}(\frac{\alpha_j}{x_2})\, \mathscr{J}_1(\alpha_j^1 x_2) - [-(\bar{\Lambda} + 2\bar{M})(\alpha_j^2) - \bar{\Lambda}\epsilon f_j^1]\, \mathscr{J}_0(\alpha_j x_2)\\
\aleph(12,k+5) &= -2\mu(\frac{\alpha_j}{x_2})\, \mathscr{J}_1(\alpha_j^1 x_2) - [-(\bar{\lambda} + 2\bar{\mu})(\alpha_j^2) + \bar{\beta} e_j - \bar{\lambda}\epsilon d_j^1]\, \mathscr{J}_0(\alpha_j x_2)\\
\aleph(13,j) &= -M((\epsilon + f_j^1))(\alpha_j^1)\, \mathscr{J}_1(\alpha_j^1 x_2)\\
\aleph(13,k+5) &= -\bar{\mu}((\epsilon + f_j^1))(\alpha_j^1)\, \mathscr{J}_1(\alpha_j^1 x_2)\\
\aleph(14,j) &= (\alpha_j^1)\, \mathscr{J}_1(\alpha_j^1 x_2),\\
\aleph(15,j) &= (d_j^1)\, \mathscr{J}_1(\alpha_j^1 x_2),\\
\aleph(16,j) &= (e_j^1)\, \mathscr{J}_1(\alpha_j^1 x_2),
\end{aligned}
$$

$\aleph(i,j)$ $i = 12,13,14,15,16$ and $j = 9,10$ and $\aleph(i,j)$ $i = 12,13$ and $j = 14,15,16$ are obtained in similar way. The non-zero elements at the other interface are $\aleph(i,j)$ $(i = 17,18,19,20,21$ and $j = 11,12,\ldots 20)$and $\aleph(i,j)$ $(i = 22,23,\ldots,28$ and $j = 19,20,\ldots 32)$and $\aleph(i,j)$ $(i = 29,30,31,32,$ and $j = 25,26,,\ldots,32)$ obtained in above mentioned way.

6 NUMERICAL DISCUSSION

The frequency equation is numerically carried out for the material PZT-5A and their material properties are given below Mahesh et al. (2021)
$C_{11} = 13.9\times10^{10} Nm^{-2}$,$C_{12} = 7.78\times10^{10} Nm^{-2}$, $C_{13} = 7.43\times10^{10} Nm^{-2}$, $C_{33} = 11.5\times10^{10} Nm^{-2}$, $C_{44} = 2.56\times10^{10} Nm^{-2}$, $T_0 = 298K$,$\rho = 5504 kgm^{-3}$, $C_T = 420 JKg^{-1}K^{-1}$, $e_{13} = -6.98 Cm^{-2}$, $e_{33} = 13.8 Cm^{-2}$, $e_{15} = -0.138 Cm^{-2}$, $\beta_1 = \beta_3 = 1.52\times10^6 Nk^{-1}m^{-2}$, $P_3 = -2.94\times10^6 Ck^{-1}m^{-2}$, $K_1 = K_3 = 1.5 Wm^{-1}K^{-1}$ $\epsilon_{11} = 60\times10^{-11} C^2N^{-1}m^{-2}$,$\epsilon_{33} = 54.7\times10^{-11} C^2N^{-1}m^{-2}$
Tab.1The Non-dimensional Frequency for real wave numbers in the first axial mode of Thermo piezoelectric hollow cylinder.

WaveNumber	Frequency		
	PZT5A	PZT/LEMV/PZT	PZT/LEMV/SWCNT/LEMV/PZT
0.2	3.1221	1.8865	1.7174
0.4	3.2033	1.9774	1.8115
0.6	3.6694	2.1413	1.9810
0.8	3.8095	2.3978	2.2451
1	3.9097	2.7108	2.5634

Tab.2 The Non dimensional Frequency for real wave numbers in the second axial mode of Thermo piezoelectric hollow cylinder.

WaveNumber	Frequency		
	PZT5A	PZT/LEMV/PZT	PZT/LEMV/SWCNT/LEMV/PZT
0.2	7.8272	6.3980	6.2289
0.4	7.8358	6.4159	6.3101
0.6	7.9137	6.4265	6.2662
0.8	7.9768	6.4625	6.1098
1	8.0965	6.5245	6.0770

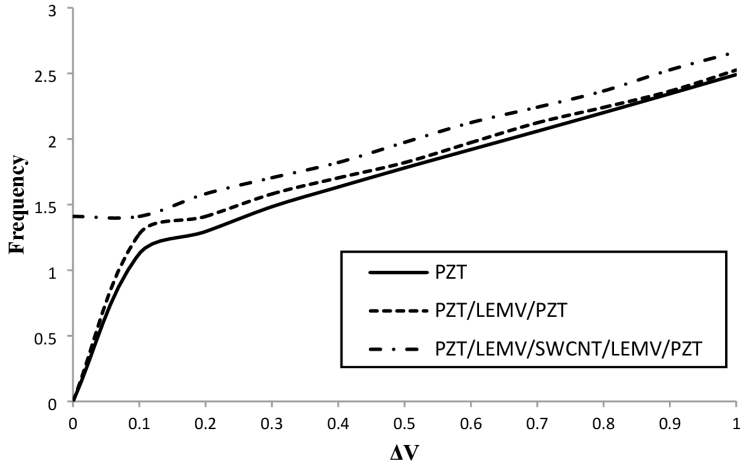

Fig. 1: Variations of the frequency of the multi layered cylinder with respect to applied electric voltage for different layers at the wave number 0.8

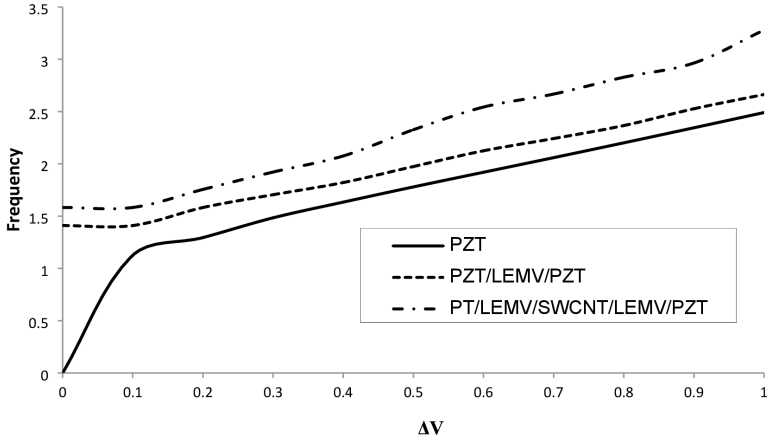

Fig. 2: Variations of the frequency of the multi layered cylinder with respect to applied electric voltage for different layers at the wave number 1.2

The frequency equations are numerically evaluated for PZT5A, PZT5A/LEMV/PZT5 and PZT5A/LEMV/SWNCT/LEMV/PZT5A composite hollow cylinder. The axisymmetric non-dimensional complex frequencies against the wave number for the first and second axial modes are given in Tables 1 and 2.From these tables non-dimensional frequency against wave number is more stable in SWNCT layer hollow cylinder compared with PZT5A and LEMV layer hollow cylinders.

In both the Fig 1 and 2, the dotted line, discontinuous line and thin line, specifies thermo piezoelectric with interfacial layers LEMV and SWNCT, LEMV and single layered thermo piezoelectric cylinders respectively. The non-dimensional frequencies against the voltage differences for different wave numbers are observed. In Fig.2 the non-dimensional frequency maintain unique nature for higher values of voltage differences but when the voltage differences is vanish the frequency in PZT5A and PZT5A/LEMV/PZT5A are also vanishes but PZT5A/LEMV/SWNCT/LEMV/PZT5A keeps certain higher magnitude due to their wave length. Similarly in Fig.2 increase the wave number from 0.8 to 1.2 yields the same results in higher values of voltage difference but voltage differences is zero the PZT layer cylinder meets zero and other two layered cylinders receipts certain value. From this observation the increasing values of wavenumber in PZT5A, PZTA/LEMV/PZT5A and PZT5A/LEMV/SWNCT/LEMV/PZT5A the non-dimensional frequency against the voltage difference maintain unique nature for higher values but deviations arise when the value is zero due to their wavelength.

Variations of the fundamental frequencies of the composite cylinder under uniform temperature rising for various compositions of layers presented in Fig.3 and 4. It can be observed that the frequencies of composite cylinder decrease with the increase of temperature change until reaches to zero at the critical temperature point. The reason of these phenomena is reduction in total stiffness of the composite cylinder, since stiffness of composite cylinder decreases when temperature changes increase. Furthermore, this treatment is different in the realm of temperature after the critical temperature. Also, uniform temperature change has a softening effect on composite cylinder at pre-buckling realm and a rise in temperature increases this effect.

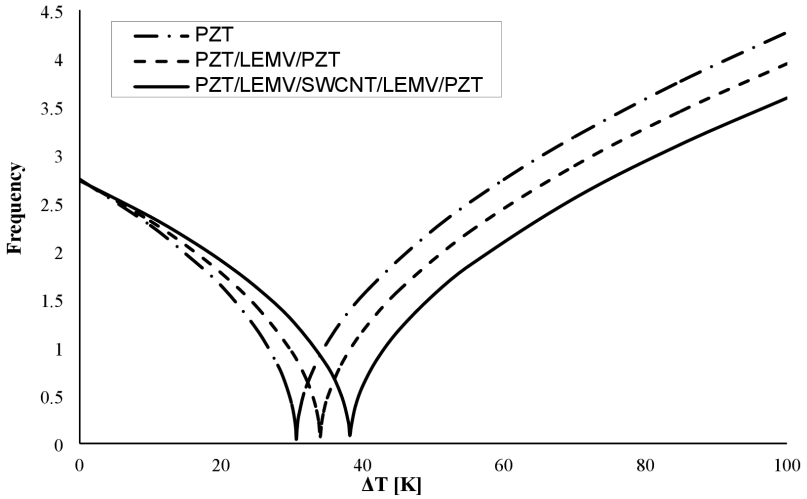

Fig. 3: Variations of the frequency of the multi layered cylinder with respect to linear temperature change for different layers at the wave number 0.8

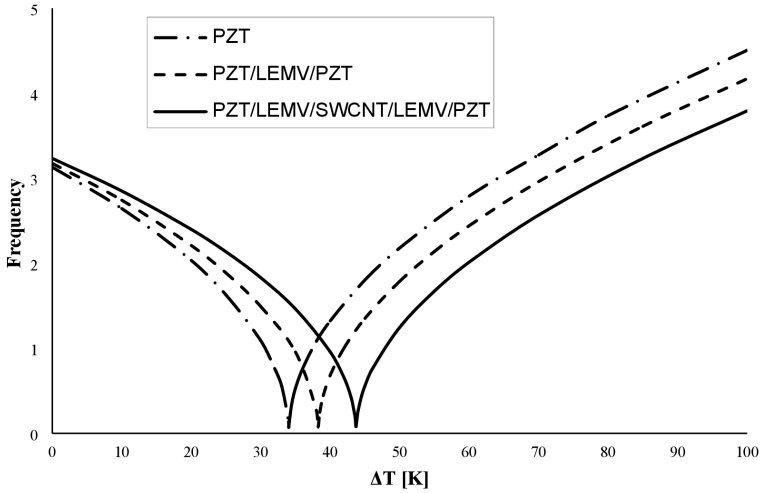

Fig. 4: Variations of the frequency of the multi layered cylinder with respect to linear temperature change for different layers at the wave number 1.2

7 Conclusion

The axisymmetric wave propagation analysis of thermo piezoelectric composite circular hollow cylinder made of interior and exterior thermo piezoelectric layer fortified together by a LEMV and SWCNT has been analyzed. Coupled partial differential equations have been found for PZT5A/LEMV/SWCNT/LEMV/PZT5A hollow circular cylinder by using linear theory of elasticity. The equations of motion, heat and electric conduction also has been exactly solved. The non-dimensional frequency has been obtained against the wavenumber, voltage difference and linear temperature change. The nature of non-dimensional frequency of PZT5A/LEMV/SWCNT/LEMV/PZT5A hollow cylinder compared with PZT5A and PZT5A/LEMV/PZT5A cylinders against the wavenumber, also voltage difference and linear temperature change for fixed wave number. The effects of this problem are very useful in the problem of dynamic response of the transversely isotropic thermo piezoelectric cylinders which has various industrial applications.

References

S Mamatha Upadhya, CSK Raju, S Saleem, AA Alderremy, et al. Modified fourier heat flux on mhd flow over stretched cylinder filled with dust, graphene and silver nanoparticles. *Results in Physics*, 9:1377–1385, 2018.

Rasool Moradi-Dastjerdi and Kamran Behdinan. Thermoelastic static and vibrational behaviors of nanocomposite thick cylinders reinforced with graphene. 2019.

Chunhui Wang, Xiaodong He, Yuanyuan Shang, Qingyu Peng, Yuyang Qin, Enzheng Shi, Yanbing Yang, Shiting Wu, Wenjing Xu, Shanyi Du, et al. Multifunctional graphene sheet–nanoribbon hybrid aerogels. *Journal of Materials Chemistry A*, 2(36): 14994–15000, 2014a.

Mohammed Sobhy. Hygrothermal vibration of orthotropic double-layered graphene sheets embedded in an elastic medium using the two-variable plate theory. *Applied Mathematical Modelling*, 40(1):85–99, 2016.

Akhil Garg, V Vijayaraghavan, CH Wong, Kang Tai, and Liang Gao. An embedded simulation approach for modeling the thermal conductivity of 2d nanoscale material. *Simulation Modelling Practice and Theory*, 44:1–13, 2014.

Kim Meow Liew, XQ He, and Sritawat Kitipornchai. Predicting nanovibration of multi-layered graphene sheets embedded in an elastic matrix. *Acta Materialia*, 54(16):4229–4236, 2006.

R Ansari, B Arash, and H Rouhi. Vibration characteristics of embedded multi-layered graphene sheets with different boundary conditions via nonlocal elasticity. *Composite Structures*, 93(9):2419–2429, 2011.

Jinbao Wang, Xiaoqiao He, Sritawat Kitipornchai, and Hongwu Zhang. Geometrical nonlinear free vibration of multi-layered graphene sheets. *Journal of Physics D: Applied Physics*, 44(13):135401, 2011.

A Sakhaee-Pour, MT Ahmadian, and R Naghdabadi. Vibrational analysis of single-layered graphene sheets. *Nanotechnology*, 19 (8):085702, 2008.

Jinbao Wang, Meiling Tian, Xiaoqiao He, and Zhibo Tang. Free vibration analysis of single-layered graphene sheets based on a continuum model. *Applied Physics Frontier*, 2(1), 2014b.

Mohammed Sobhy. Generalized two-variable plate theory for multi-layered graphene sheets with arbitrary boundary conditions. *Acta Mechanica*, 225(9):2521–2538, 2014.

Farzad Ebrahimi and Navvab Shafiei. Influence of initial shear stress on the vibration behavior of single-layered graphene sheets embedded in an elastic medium based on reddy's higher-order shear deformation plate theory. *Mechanics of Advanced Materials and Structures*, 24(9):761–772, 2017.

Hamidreza Bakhshalizadeh and Majid Ghadiri. Size-dependent vibration behavior of graphene sheet with attached spring-mass and damper system based on the nonlocal eringen theory. *Mechanics of Advanced Materials and Structures*, pages 1–10, 2020.

Olga Mazur and Jan Awrejcewicz. Ritz method in vibration analysis for embedded single-layered graphene sheets subjected to in-plane magnetic field. *Symmetry*, 12(4):515, 2020.

Kamran Kamali and Reza Nazemnezhad. A novel method for considering interlayer effects between graphene nanoribbons and elastic medium in free vibration analysis. *Mechanics of Advanced Composite Structures*, 7(1):79–88, 2020.

HR Analooei, M Azhari, S Sarrami-Foroushani, and A Heidarpour. On the vibration and buckling analysis of quadrilateral and triangular nanoplates using nonlocal spline finite strip method. *Journal of the Brazilian Society of Mechanical Sciences and Engineering*, 42(4):1–14, 2020.

Kamran Behdinan, Rasool Moradi-Dastjerdi, Babak Safaei, Zhaoye Qin, Fulei Chu, and David Hui. Graphene and cnt impact on heat transfer response of nanocomposite cylinders. *Nanotechnology Reviews*, 9(1):41–52, 2020.

Farzad Ebrahimi, Pendar Hafezi, and Ali Dabbagh. Buckling analysis of embedded graphene oxide powder-reinforced nanocomposite shells. *Defence Technology*, 17(1):226–233, 2021.

Rasool Moradi-Dastjerdi and Kamran Behdinan. Stability analysis of multifunctional smart sandwich plates with graphene nanocomposite and porous layers. *International Journal of Mechanical Sciences*, 167:105283, 2020.

Farzad Ebrahimi and Ali Dabbagh. Viscoelastic wave propagation analysis of axially motivated double-layered graphene sheets via nonlocal strain gradient theory. *Waves in Random and Complex Media*, 30(1):157–176, 2020.

Mustapha Fouaidi, Abdellah Hamdaoui, Mohammad Jamal, and Bouazza Braikat. Numerical analysis of single-layered graphene sheets by a mesh-free approach. *Engineering with Computers*, 37(3):2193–2206, 2021.

Moussa Bellal, Habib Hebali, Houari Heireche, Abdelmoumen Anis Bousahla, Abdeldjebbar Tounsi, Fouad Bourada, SR Mahmoud, EA Adda Bedia, and Abdelouahed Tounsi. Buckling behavior of a single-layered graphene sheet resting on viscoelastic medium via nonlocal four-unknown integral model. *Steel and Composite Structures, An International Journal*, 34(5):643–655, 2020.

Zahra Shafiei, Saeid Sarrami-Foroushani, Fatemeh Azhari, and Mojtaba Azhari. Application of modified couple-stress theory to stability and free vibration analysis of single and multi-layered graphene sheets. *Aerospace Science and Technology*, 98:105652, 2020.

Cheng Hui Xu, Jing Jing Hu, and Da Lun Rong. Flexural wave propagation of double-layered graphene sheets based on the hamiltonian system. In *Materials Science Forum*, volume 975, pages 121–126. Trans Tech Publ, 2020.

R Selvamani and S Mahesh. Mathematical modeling and analysis of elastic waves in a thermo piezoelectric multilayered rotating composite rod with lemv/cfrp interface. *Technische Mechanik-European Journal of Engineering Mechanics*, 39(3):241–251, 2019.

Stephen C Cowin and Jace W Nunziato. Linear elastic materials with voids. *Journal of elasticity*, 13(2):125–147, 1983.

Mira Mitra and S Gopalakrishnan. Vibrational characteristics of single-walled carbon-nanotube: Time and frequency domain analysis. *Journal of applied physics*, 101(11):114320, 2007.

S Mahesh, R Selvamani, and F Ebrahami. Assessment of hydrostatic stress and thermo piezoelectricity in a laminated multilayered rotating hollow cylinder. *Mechanics of Advanced Composite Structure*, 8(1):77–86, 2021.